

Identification of FGF10 Targets in the Embryonic Lung Epithelium during Bud Morphogenesis*

Received for publication, September 16, 2004, and in revised form, November 16, 2004
Published, JBC Papers in Press, November 19, 2004, DOI 10.1074/jbc.M410714200

Jining Lü, Konstantin I. Izvolsky, Jun Qian, and Wellington V. Cardoso‡

From the Pulmonary Center, Boston University School of Medicine, Boston, Massachusetts 02118

Genetic studies implicate Fgf10-Fgfr2 signaling as a critical regulator of bud morphogenesis in the embryo. However, little is known about the transcriptional targets of Fgf10 during this process. Here we identified global changes in gene expression in lung epithelial explants undergoing FGF10-mediated budding in the absence of other growth factors and mesenchyme. Targets were confirmed by their localization at sites where endogenous Fgf10 signaling is active in embryonic lungs and by demonstrating their induction in intact lungs in response to local application of FGF10 protein. We show that the initial stages of budding are characterized by marked up-regulation of genes associated with cell rearrangement and cell migration, inflammatory process, and lipid metabolism but not cell proliferation. We also found that some genes implicated in tumor invasion and metastatic behavior are epithelial targets of Fgf10 in the lung and other developing organs that depend on Fgf10-Fgfr2 signaling to properly form. Our approach identifies Fgf10 targets that are common to multiple biological processes and provides insights into potential mechanisms by which Fgf signaling regulates epithelial cell behavior.

The spatial and temporal distribution of Fgf10 is essential for patterning of lung epithelial tubules.

Bud morphogenesis involves major changes in cytoskeletal organization, cell adhesion, migration, invasion, and proliferation among other activities. Little is known about the targets of Fgf10-Fgfr2b signaling in the lung epithelium when buds are forming. Although gene expression in the developing lung has been characterized by several reports, most studies were performed in the intact organ. Using whole lungs to identify targets that result primarily from Fgf10-Fgfr2b activation is difficult, because in the mesoderm, Fgf10 is present with several other endogenous signals such as Wnts, hepatocyte growth factor, or epidermal growth factor.

Previous studies have shown that recombinant FGF10 is able to support bud morphogenesis of E11.5 lung epithelial explants in Matrigel in the absence of mesenchyme or serum (10). Here we used mesenchyme-free epithelial cultures to investigate global changes in gene expression induced by FGF10 during the initiation of budding. Our approach identifies a large number of genes not previously known to be present in the lung epithelium during bud morphogenesis or responsive to Fgf10. Among them were genes associated with cell rearrangement and cell migration, inflammatory processes, lipid metabolism, and tumor invasion. Our data provide insights into potential mechanisms by which Fgf10-Fgfr2b orchestrates bud morphogenesis in the lung and presumably in other organs.

EXPERIMENTAL PROCEDURES

Mesenchyme-free Epithelial Cultures—Lung epithelial explants from E11.5 CD-1 mice (Charles River Laboratories) were isolated from the surrounding mesenchyme after Dispase digestion (37 °C for 15 min, Roche Applied Science), embedded in growth factor-reduced Matrigel (R&D Systems), and cultured in serum-free Dulbecco's modified Eagle's medium (Invitrogen) supplemented with 2500 ng/ml human recombinant FGF10 (R&D Systems) as described (Fig. 1A) (10). Cultures were harvested after 8 or 24 h for isolation of total RNA.

Whole Lung Organ Cultures—E11.5 intact lungs were cultured in BGJb medium (Invitrogen, 20 mg/100 ml ascorbic acid, 1% inactivated fetal calf serum), as described previously (10). For some cultures, heparin beads soaked in either buffer (PBS) or FGF10 (100 ng/μl, R&D Systems) were engrafted near distal buds. Cultures were harvested at 48 or 72 h, fixed in 4% paraformaldehyde, and processed for paraffin embedding or whole mount *in situ* hybridization.

RNA Isolation, Amplification, Microarray Hybridization, and Analysis—Total RNA was isolated from mesenchyme-free lung epithelial explants at 0, 8, and 24 h using RNeasy kit (Qiagen). RNA was submitted to one-round amplification (Ribo Amp RNA amplification kit, Arcturus), labeled, and hybridized to chips using the Affymetrix kit according to manufacturer's instructions.

Two sets of arrays (Affymetrix, MG-U74v2 set) were hybridized per sample at each time point. The background signal for each array was <100 within the recommendation limit. Preferential amplification of 3'-gene regions was observed in all of the samples; glyceraldehyde-3-phosphate dehydrogenase 3'/5' ratio ranged from 14 to 19 (over a 4.0-fold recommendation limit). Affymetrix Microarray Suite, version 5.0 was used with a global scaling factor of 500 to acquire the target intensity. The scaling factors used to normalize the target value were

AQ: A

AQ: B

AQ: C

Fn1

Signaling by fibroblast growth factor 10 (Fgf10)¹ and its receptor Fgfr2b is critical for bud morphogenesis in many developing structures. During organogenesis, Fgf10 is expressed by the mesoderm from where it diffuses to activate Fgfr2b in adjacent endodermal or ectodermal-derived cells and induce budding (1). Disruption of Fgf10-Fgfr2b signaling is lethal at birth and results in multiple organ defects. Abnormalities in *Fgf10*- or *Fgfr2b*-deficient mice include agenesis of the anterior pituitary gland, lung, thyroid, salivary gland, and limb and dysgenesis of inner ear, teeth, skin, pancreas, kidney, palate, and hair follicles (2–5). Fgf10 expression is also required for adipocyte differentiation and wound healing (6–8).

In the developing respiratory tract of the mouse, *Fgf10* was first detected at embryonic (E) day 9.5 during primary bud formation. Subsequently, during branching morphogenesis (E10.5–16.5), *Fgf10* was dynamically expressed in the distal lung mesenchyme at the prospective sites of budding (9, 10).

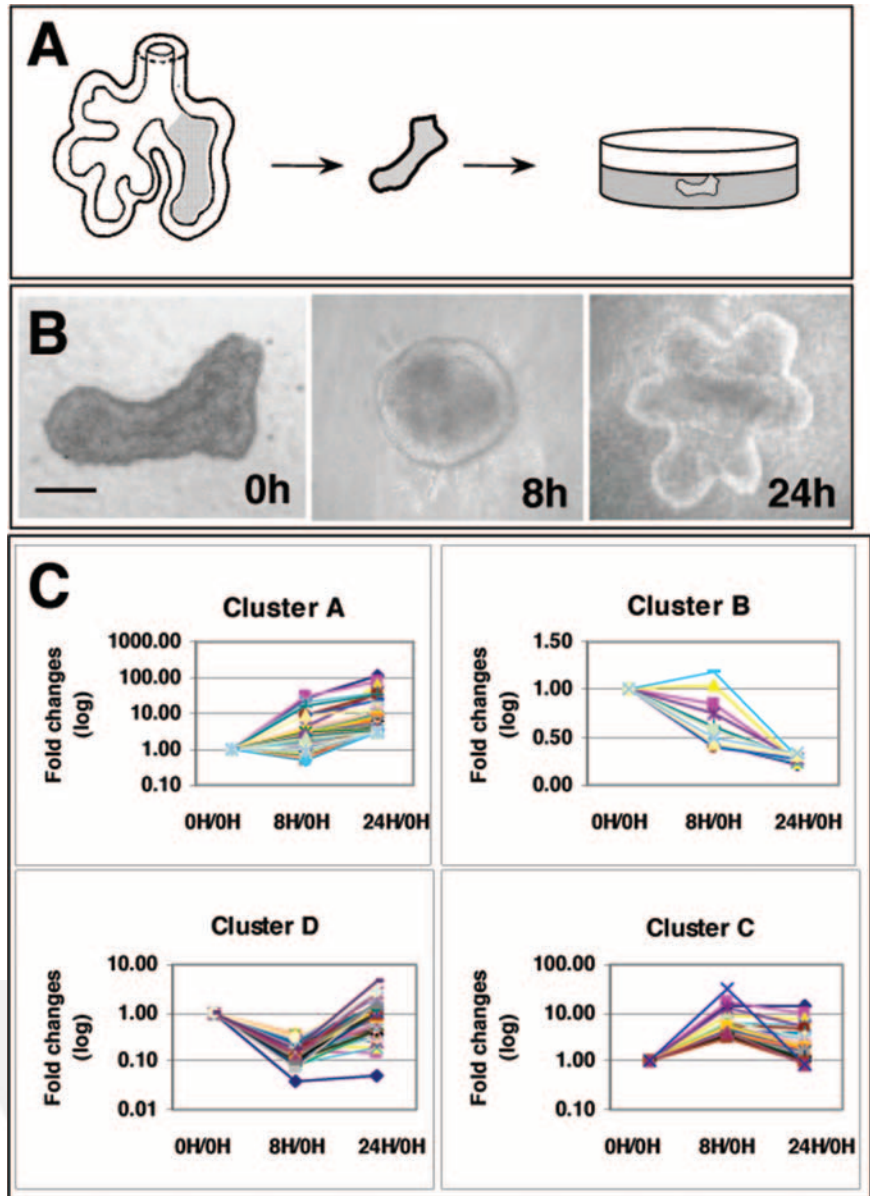
* This work was supported by Grant (PO1) HL47049 from the NHLBI, National Institutes of Health. The costs of publication of this article were defrayed in part by the payment of page charges. This article must therefore be hereby marked "advertisement" in accordance with 18 U.S.C. Section 1734 solely to indicate this fact.

‡ To whom correspondence should be addressed: Pulmonary Center, Boston University School of Medicine, 80 E. Concord St., R-304, Boston, MA 02118. Tel.: 617-638-6198; Fax: 617-536-8093; E-mail: wcardoso@lung.bumc.bu.edu.

¹ The abbreviations used are: Fgf or FGF, fibroblast growth factor; fgfr, fgf receptor; E, embryonic day; C/EBPα, CCAAT-enhancer binding protein α; PBS, phosphate-buffered saline; Bmp, bone morphogenetic protein.

AQ: K, L

FIG. 1. A, diagram illustrates methodology for culturing mesenchyme-free lung epithelial explants. E11.5 lung epithelium (*left*) is separated from the mesenchyme, embedded in Matrigel, and cultured in serum-free medium (*right*). B, whole mount explants at 0, 8, and 24 h in culture (*bar* represents 250 μ M). C, microarray analysis of mesenchyme-free lung epithelial explants at 0, 8, and 24 h in culture in the presence of FGF10. Clustering of genes with similar trends in expression during FGF10-induced budding. *Cluster A*, genes up-regulated in time; *Cluster B*, genes down-regulated in time; *Cluster C*, initial increase followed by stabilization or decrease in expression; *Cluster D*, initial down-regulation followed by a recovery in expression. Changes are represented in logarithmic scale and in hours.



within 4-folds of each other for all comparisons (range from 0.51 to 2.16). Genes for which detection *p* value was greater than 0.01 (absent call) in all six samples were discarded. Fold changes and *p* values were determined for three comparisons: 0–8; 8–24; and 0–24 h. The *Gene Cluster* (the laboratory of Michael Eisen) and *EASE* (SAIC-Frederick, Inc.) software were used to group genes with similar trends in expression and to find representation of GO categories, respectively.

In Situ Hybridization—Whole mount *in situ* hybridization of freshly isolated E11.5 lungs or lung cultures was performed in 96-well plates as described previously (11). Isotopic *in situ* hybridization was performed as described previously (12). Some cDNA clones used for probe labeling were obtained from NIA Mouse 15K cDNA clone set (Tufts University School of Medicine). The GenBank™ accession numbers were: *Perp* (BG078591); *Catnb* (BG065470); *Tm4sf3* (BG065758); *Lmo7* (BG066247); *Tacstd2* (BG066797); *Tgtp* (BG067921); *Porimin* (BG074161); and *Lrpap1* (BG075378). Others were generated by PCR using GenBank™ sequences as described previously (13) as follows: *Anxa1* 5' primer, 5'-AATTAACCTCACTAAAGGTTGAGAAGTGCCTCACACCA-3'; *Anxa1* 3' primer, 5'-TAATACGACTCACTATAGGAGACTTATCTGCCAAAGCAAC-3'; *Anxa3* 5' primer, 5'-AATTAACCTCACTAAAGGATCTTTCACTTCGCTGAGCT-3'; *Anxa3* 3' primer, 5'-TAATACGACTCACTATAGGTTTCTTCAGTTCGTTTCGATC-3'; *Timp3* 5' primer, 5'-AATTAACCTCACTAAAGGGCATGTATACACCTCTTCT-3'; *Timp3* 3' primer, 5'-TAATACGACTCACTATAGGACTCTCAGTCTGTCTCTT-3'; *Bmpr1a* 5' primer, 5'-AATTAACCTCACTAAAGGCGTGAGGTTGTGTGTGAA-3'; *Bmpr1a* 3' primer, 5'-TAATACGACTCACTATAGGACTGTTAGCA-

GCCTGTGAAGA-3'; *Saa3* 5' primer, 5'-AATTAACCTCACTAAAGGGGAAGCCTTCCATTGCCATCAT-3'; *Saa3* 3' primer, 5'-TAATACGACTCACTATAGGGGGATGTTTAGGGATCCAGAT-3'; *Vnn1* 5' primer, 5'-AATTAACCTCACTAAAGGGTCTGAGAAGCGAGCAGATGA-3'; *Vnn1* 3' primer, 5'-TAATACGACTCACTATAGGGTTCCCATACAACCTCCCAA-3'; *Myh7* 5' primer, 5'-AATTAACCTCACTAAAGGGGAAGAACATGGAGCAGACCAT-3'; and *Myh7* 3' primer, 5'-TAATACGACTCACTATAGGGAGCACAAAGATCTACTCCTCAT-3'.

RESULTS AND DISCUSSION

Global Trends in Gene Expression in FGF10-treated Epithelial Cultures

We assessed gene expression in the lung epithelium during the initial stages of bud formation *in vitro* without intervening signals from the mesenchyme and having FGF10 as the sole growth factor in the medium. Within the initial 8 h in culture (pre-budding stage), the epithelial tube seals, presumably by a mechanism reminiscent of wound healing. By 24 h, a first generation of buds becomes evident (onset budding) (Fig. 1B). Subsequent stages (48 h, not studied here) are characterized by bud elongation and by the appearance of a second generation of buds. *Fgfr2b* was expressed at all times. The explants were unable to survive without exogenous FGF10 (Matrigel alone).

F1

FGF10 Targets during Bud Morphogenesis

3

TABLE I
Representative genes from each cluster

N.D., not done in this study; ISH, *in situ* hybridization.

Symbols/accession no.	Protein encoded/homolog	Fold change			Biological function	ISH confirmation
		8H/0H	24H/0H	24H/8H		
Cluster A						
<i>Tgtp</i>	T-cell-specific GTPase	3.95	59.66	15.1	Signal transduction	Fig. 2A
<i>Numb</i>	numb gene homolog (<i>Drosophila</i>)	2.41	4.33	1.8	Signal transduction	N.D
<i>Bmpr1a</i>	bone morphogenetic protein receptor, type 1A	2.14	10.94	5.12	Signal transduction	Fig. 2G
<i>Catnb</i>	β -catenin	1.12	3.15	2.83	Signal transduction	N.D
<i>Tacstd2</i>	Tumor-associated calcium signal transducer 2	16.48	32.1	1.95	Signal transduction	Fig. 2B
<i>Tm4sf3</i>	transmembrane 4 superfamily member 3	3.4	10.52	3.09	Signal transduction	Fig. 2C
<i>Vnn1</i>	vanin 1	1.45	9.81	6.75	Cell motility	Fig. 2H
<i>Myh7</i>	myosin, heavy polypeptide 7, cardiac muscle, β	29.41	78.48	2.67	Cell motility	Fig. 2I
<i>Myhca</i>	myosin heavy chain, cardiac muscle, adult	1.74	3.9	2.24	Cell motility	N.D
<i>Tmod3</i>	Tropomodulin 3	1.99	4.05	2.04	Cell motility	N.D
<i>Anxa1</i>	annexin A1	26.42	110.33	4.18	Inflammation	Fig. 2D
<i>Anxa3</i>	annexin A3	19.75	35.92	1.82	Inflammation	Fig. 2J
<i>S100a13</i>	S100 calcium-binding protein A13	2.47	3.22	1.3	Inflammation	N.D
<i>Anxa2</i>	annexin A2	2.15	4.22	1.96	Inflammation	N.D
<i>Saa3</i>	Serum amyloid A 3	9.36	35.14	3.75	Inflammation	Fig. 2K
<i>Ager</i>	advanced glycosylation end product-specific receptor	0.96	3.46	3.6	Inflammation	N.D
<i>Il10rb</i>	interleukin 10 receptor, β	1.68	4.02	2.4	Inflammation	N.D
<i>Cdh16</i>	Cadherin 16	0.68	4.82	7.14	Cell adhesion	Data not shown
<i>Ahnak</i>	AHNAK nucleoprotein (desmoyokin)	8.56	24.6	2.87	Cell adhesion	N.D
<i>3732412D22Rik</i>	Similar to LIM domain only 7	0.54	4.1	7.62	Proteolysis	N.D
<i>Ctsh</i>	Cathepsin H	4.46	35.78	8.02	Proteolysis	Data not shown
<i>Lmo7</i>	LIM domain only 7	2.31	14.01	6.06	Proteolysis	Fig. 2L
<i>Timpp3</i>	tissue inhibitor of metalloproteinase 3	3.13	9.31	2.98	Proteolysis	Fig. 2E
<i>Lrpap1</i>	HBP44	0.55	5.05	9.13	Heparin binding	Fig. 2F
<i>Perp-pending</i>	p53 apoptosis effector related to Pmp22	8.4	12.91	1.54	Apoptosis	Fig. 2M
<i>Prkdc</i>	protein kinase, DNA-activated, catalytic polypeptide	2.7	10.21	3.78	DNA-binding kinase	Data not shown
<i>Cyp1b1</i>	cytochrome P450, 1b1, benz[a]anthracene-inducible	1.71	15.31	8.96	Metabolism	Fig. 2N
<i>2310075C12Rik</i>	PORIMIN (human homolog)	0.74	3.59	4.83	Cell death	Fig. 2O
Cluster B						
<i>Rex3</i>	Reduced expression 3	1.05	0.23	0.22	Unknown	Ref. 13
<i>Jun</i>	Jun oncogene	0.58	0.3	0.52	Transcription	N.D
<i>Ncl</i>	Nucleolin	0.5	0.33	0.65	Transcription	N.D
Cluster C						
<i>Cdkn1a</i>	Cyclin-dependent kinase inhibitor 1A (P21)	5.83	1.91	0.33	Mitotic cell cycle	N.D
<i>Ache</i>	Acetylcholinesterase	6.54	3.16	0.48	Mitotic cell cycle	N.D
<i>Akap8</i>	A kinase (PRKA) anchor protein 8	3.19	1	0.31	Mitotic cell cycle	N.D
<i>Ldlr</i>	Low density lipoprotein receptor	3.14	0.97	0.31	Lipid metabolism	N.D
<i>Hsd3b2</i>	Hydroxysteroid dehydrogenase-2, $\Delta<5>-3-\beta$	3.83	1.8	0.47	Lipid metabolism	N.D
<i>Lss</i>	Lanosterol synthase	3.4	1.54	0.45	Lipid metabolism	N.D
<i>HSL</i>	Lipase, hormone sensitive	12.43	5.04	0.41	Lipid metabolism	N.D
<i>Cyp51</i>	Cytochrome P450, 51	3.96	2.25	0.57	Lipid metabolism	N.D
<i>Scd1</i>	Stearoyl-Coenzyme A desaturase 1	3.88	3	0.77	Lipid metabolism	N.D
<i>Nupr1</i>	Nuclear protein 1	32.24	0.83	0.03	Transcription	N.D
<i>S100a6</i>	S100 calcium-binding protein A6 (calcyclin)	3.27	3.28	1	Inflammation	N.D
Cluster D						
<i>Atp5l</i>	ATP synthase, subunit g	0.16	0.38	2.4	Nucleotide biosynthesis	N.D
<i>Ctsz</i>	Cathepsin Z	0.3	0.57	1.94	Endopeptidase	N.D
<i>Ccnb1</i>	Cyclin B1	0.26	0.48	1.86	Cell cycle	N.D
<i>Sftpc</i>	Surfactant-associated protein C	0.28	0.32	1.15	Respiratory gas exchange I	N.D

219 genes were selected for further analysis based on the following criteria: fold changes equal or over 3.0 with a p value <0.05 in at least one of the comparisons. Representative genes are shown in Table I. Four major clusters of regulated genes were defined based on how their levels of expression changed in time (Fig. 1C).

Cluster A—Cluster A consisted of 68 genes (31% of the 219 selected) with a steady increase in expression levels from 0 to 24 h in culture. This trend correlated positively with the increasing budding activity of the cultured epithelium. Genes implicated in signal transduction, cell motility, inflammation-repair responses, and genes associated with cellular membranes were overrepresented (Table II). They were probably FGF10 targets induced to promote healing of the explants and to initiate bud formation.

Cluster B—Cluster B comprised 13 genes (~6%) whose expression declined in culture from 0 to 24 h. Gene categories

related to transcription and oxidoreductase activity were over-represented (Table II). The expression of these genes may have been repressed by FGF10 or, alternatively, could not be maintained in culture without other mesenchymal signals. For example, in the intact E11.5 lung, *Rex3* (repressed by retinoic acid 3) was known to be strongly expressed in the distal epithelium (13) where *Fgf10* signaling is active. However, in our cultures, *Rex3* was clearly down-regulated despite the presence of exogenous FGF10.

Cluster C—Cluster C included 31 genes (14%) up-regulated within the initial 8 h and subsequently down-regulated or without further change in levels from 8 to 24 h. This cluster was overrepresented in genes involved in mitotic cell cycle and steroid and lipid metabolism. Among them were the well characterized stress-induced genes *Nupr1* (nuclear protein 1 or *p8*), *Ache* (acetylcholinesterase), *Hspa1b* (heat shock protein 1B), and *Procr* (protein C receptor, endothelial). The remarkable

T1

T2

FGF10 Targets during Bud Morphogenesis

TABLE II
Overrepresented GO categories in each cluster

Cluster A	GO biological process Response to external stimulus Cell motility Blood coagulation Inflammatory response Protein amino acid glycosylation	GO cellular component Integral to membrane Microsome Endoplasmic reticulum membrane	GO molecular function Calcium ion binding Enzyme inhibitor activity Phospholipase inhibitor activity Monooxygenase activity
Cluster B			DNA binding Oxidoreductase activity
Cluster C	Oncogenesis Steroid metabolism Glycoprotein metabolism Mitotic cell cycle		Protein kinase regulator activity
Cluster D	Isoprenoid metabolism Nucleotide biosynthesis Nucleotide biosynthesis Steroid biosynthesis Carbohydrate metabolism Biosynthesis Coenzyme and prosthetic group metabolism M phase of mitotic cell cycle Negative regulation of transcription from Pol II promoter	Mitochondrial large ribosomal subunit Ribosome Cytoplasm Vacuole Intracellular Mitochondrion Mitochondrial matrix Ribonucleoprotein complex	DNA topoisomerase activity Oxidoreductase activity Cysteine-type peptidase activity ATP binding Steroid binding Hydrolase activity

transient up-regulation of *Nupr* observed during the initial 8 h in culture (32-fold) may, at least in part, represent a response of the explant to the dramatic changes in the environment (14).

Cluster D—Cluster D comprised 107 genes (49%) whose expression declined during the initial 8 h, but returned to normal levels by 24 h in culture. Cluster D was overrepresented in gene categories related to nucleotide biosynthesis, ATP binding, metabolism and biosynthesis, DNA repair, M-phase mitosis, and cysteine-type endopeptidase activity. Expression of these genes may have been initially affected by environmental factors, but it recovered subsequently.

In situ hybridization analysis of E11.5 lungs confirmed epithelial expression of 22 of 26 uncharacterized genes. Most showed increased signals in distal epithelium where endogenous Fgf10 is active (Fig. 2, *Group I*). Nine genes were additionally expressed in distal mesenchyme (Fig. 2, *Group II*). Inducibility by FGF10 was confirmed for 16 of 20 genes by detection of strong signals in the epithelium associated with beads loaded with FGF10 engrafted in whole lung cultures (Figs. 3 and 4, *E–G* and *P–R*).

Known Signaling Pathways Influenced by Fgf10 during Bud Morphogenesis

Activation of Fgf10-Fgr2b signaling has been shown to influence the expression of other Fgfs, Bmps, Wnt- β -catenin, and Shh (Sonic hedgehog) in a variety of developing structures. We found that within the initial 24 h of budding, only two components of these pathways (*Bmpr1a* and *Catnb*) were clearly up-regulated by FGF10.

Bmpr1a, which encodes type I receptor for BMP, showed an 11-fold increase in expression (0–24 h). *Bmp4* is a well known target of Fgf10 in branching epithelial tubules where it is believed to control Fgf-mediated bud outgrowth. Studies in lung explant culture systems demonstrate that FGF10 induction of *Bmp4* is evident only by 48 h of treatment (15, 16). Consistent with this finding, we could not detect significant changes in *Bmp4* levels within the 0–24-h period. However, its receptor was markedly up-regulated by 24 h (Table I). Figs. 2*G* and 3*A* show *Bmpr1a* expression in the distal lung epithelium and its up-regulation by local FGF10. Sequential induction of *Bmpr1a* and *Bmp4* by FGF10 probably underlies a mechanism by which Bmp signaling is established in the lung bud to limit the FGF10 effects. Hence, FGF10 initially

induced the expression of *Bmpr* in the nascent bud to make it competent to respond to a BMP signal that would be induced in a subsequent step.

β -catenin (*Catnb*) is a key component of the Wnt pathway and the cell adhesion-cadherin complex expressed throughout the epithelium of the developing lung (17, 18). We found a 3-fold increase in *Catnb* transcripts (0–24 h, Table I), but no obvious induction of known Wnt ligands or targets was present in the array. Notably, the Wnt receptor *Fzd2* (Frizzled 2) was down-regulated (2.5-fold) by 24 h. Activation of Fgf10-Fgr2b or the *Wnt-Catnb* canonical pathways maintains multipotency of progenitor cells in several developing structures (19). Interestingly, in the embryonic chick skin, Fgf10 can increase *Catnb* protein levels and exert its effect on progenitor cells independent of Wnt activation (20). Although in our system we cannot rule out activation of the Wnt signaling, it is possible that *Catnb* expression may be similarly regulated by FGF10 in lung progenitors during bud morphogenesis.

FGF10 Induces Genes That Regulate Cell Polarity, Adhesion, and Directed Cell Migration

Polarized cell migration was initiated with lamellipodia formation, a process that is dependent on Fgf signaling (21). Our screen revealed increased expression of a large number of genes associated with cell adhesion, cytoskeleton activity, and cell polarity during the initial 24-h period of budding. These included the following: *Tm4sf3* (transmembrane 4 superfamily 3) (10-fold increase, Figs. 2*C* and 4), a tetraspanin molecule that associates with integrins to control lamellipodia formation (22); *Numb* (4.3-fold, Table I), a component of the *Drosophila* planar polarity signaling that regulates epithelial cell polarity (23); and *Tmod3*, (Tropomodulin-3) (4-fold, Table I), an actin filament pointed end-capping protein that, in excess, inhibits lamellipodia protrusion and cell motility (24); and *Vnn1* (Vannin-1) (9.8-fold, Fig. 2*H*), which encodes a GPI-anchored protein possibly implicated in cell migration in the thymus and in mammalian sexual development (25, 26).

Other genes involved in cell-cell or cell-substrate adhesion significantly up-regulated were as follows: *Lmo7* (LIM domain 7) (14-fold, Fig. 2*L*), an afadin- and α -actinin-binding protein implicated in assembly of epithelial adherens junctions (27), and *Cdh16* (cadherin 16) (4.8-fold, Table I), a cell adhesion molecule previously reported in the developing kidney and lung

F2

F3

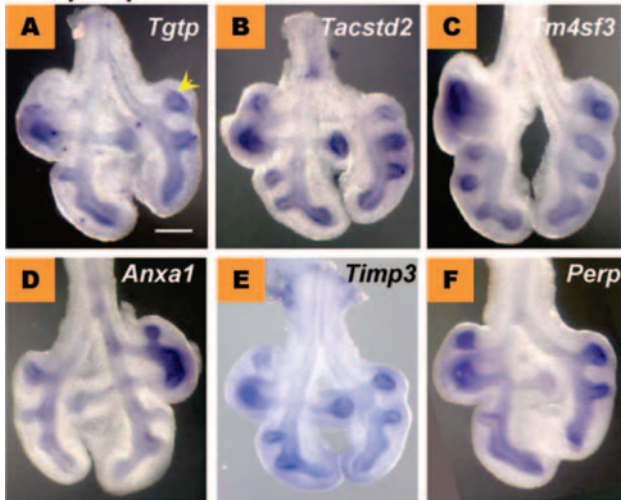
F4

AQ: E

FGF10 Targets during Bud Morphogenesis

5

Group I: epithelium



Group II: epithelium and mesenchyme

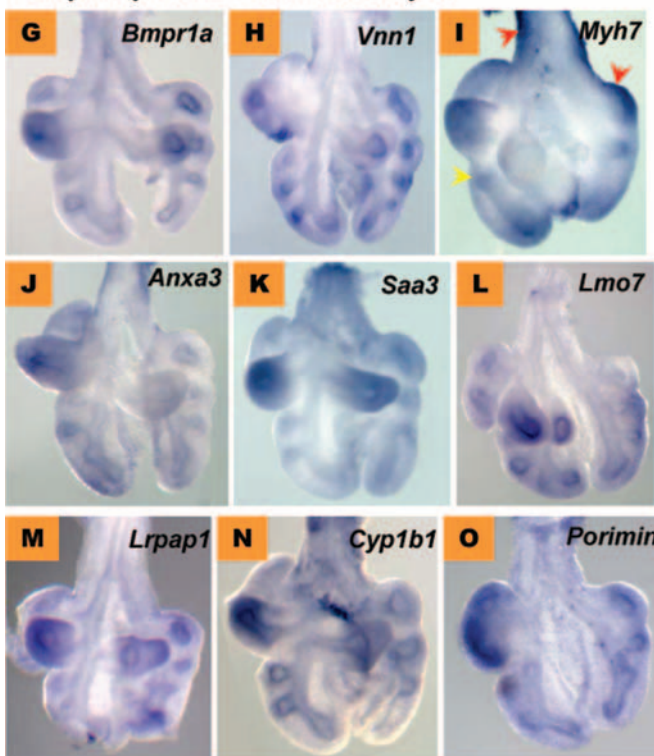


FIG. 2. Whole mount *in situ* hybridization confirmation of genes from Cluster A in E11.5 mouse lungs. Group I, expression in epithelium (yellow arrow): *Tgtp* (A); *Tacstd2* (B); *Tm4sf3* (C); *Anxa1* (D); *Timp3* (E); and *Perp* (F). Group II, expression in both epithelium (yellow arrow) and mesenchyme (red arrow): *Bmpr1a* (G); *Vnn1* (H); *Myh7* (I); *Anxa3* (J); *Saa3* (K); *Lmo7* (L); *Lrpap1* (M); *Cyp1b1* (N); and *Porimin* (O). Scale bar in A = 250 μ m.

epithelium with function not yet characterized (28).

An unexpected finding was *Myh7* (myosin, heavy polypeptide-7, β -cardiac muscle) transcripts in the epithelial explants and its striking up-regulation by FGF10 (79-fold). In humans, 18 classes of myosins have been described in muscular or epithelial structures. During epithelial morphogenesis, some myosins (class II) play a role in epithelial cell intercalation, polarization, and focal adhesion (29). *Myh7* has been reported in mouse mesodermal cells of the developing heart and somites but not in epithelial structures (30). *In situ* hybridization of E11–12 lungs showed *Myh7* signals in distal epithelial buds and surrounding mesenchyme where *Fgf10* is expressed (Fig.

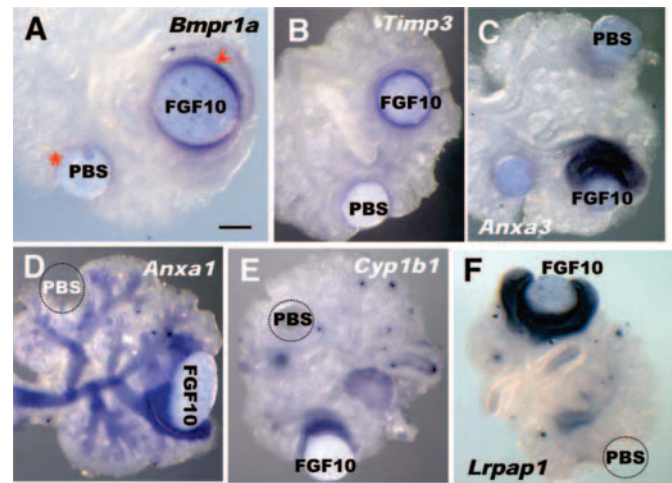


FIG. 3. Gene inducibility by FGF10 as confirmed by *in situ* hybridization of whole lung organ cultures at 48 h. Strong gene expression (arrow) is induced in the epithelium associated with an FGF10 but not a PBS (control) bead (asterisk). A, *Bmpr1a*. B, *Timp3*. C, *Anxa3*. D, *Anxa1*. E, *Cyp1b1*. F, *Lrpap1*. Scale bar in A = 300 μ m.

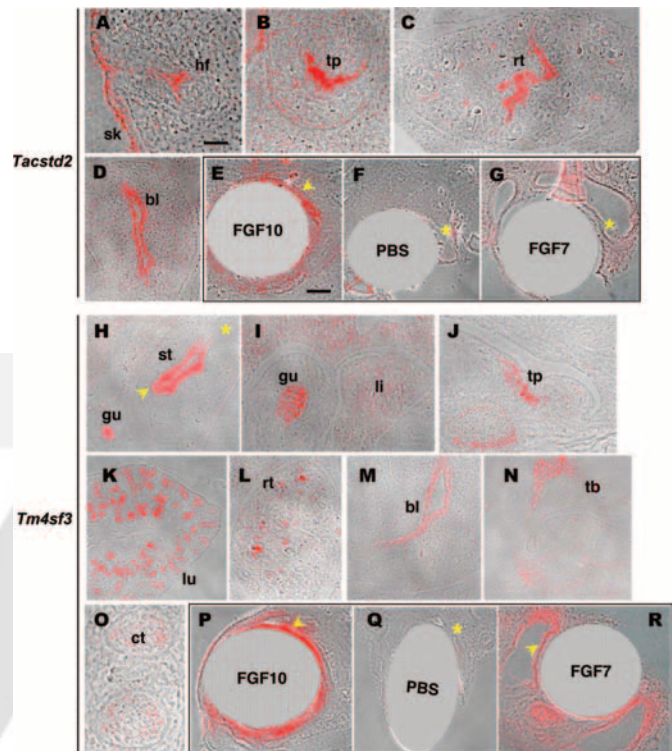


FIG. 4. Isotopic *in situ* hybridization of tumor-associated FGF10 targets during organogenesis. A–G, *Tacstd2* expression at E14 in ectodermal layer of the skin (*sk*) and epithelial structures of the hair follicle (*hf*) (A), tooth primordium (*tp*) (B), renal tubules (*rt*) (C), and urogenital sinus of future bladder (*bl*) (D). In lung organ cultures, *Tacstd2* is up-regulated by FGF10 (E) but not by FGF7 (G) or PBS beads (F). H–T, *Tm4sf3* expression in epithelia of E12 stomach (*st*, note anterior-posterior gradient) and gut (*gu*) (H), in epithelia of E14 gut and liver (*li*) (I), lung (*lu*) (K), renal tubules (*rt*) (L), bladder (M), tooth primordium (*tp*) (J), and in mesenchymal tissues such as turbinates (*tb*) (N), and cartilage (*ct*) (O). In contrast to *Tacstd2*, *Tm4sf3* is up-regulated by either FGF10 or FGF7 beads in lung organ cultures. PBS beads show no effect (P–R). Arrows depict high level signals. Asterisks depict lack of signals. Scale bar in A = 100 μ m; scale bar in E = 30 μ m. FC, fold change; N.D., not done in this study; ISH, *in situ* hybridization.

AQ: M

2I). Transcripts were also seen in proximal mesenchyme in association with developing vascular or muscular structures. Another cardiac myosin (α , *Myh6*) gene was also up-regulated in our array ($p < 0.05$) but to a lesser degree (3.9-fold, Table I).

We had no evidence of mesenchymal cell contamination, because expression of other cardiac genes or vimentin was undetectable. Interestingly, a similar study in rat mesenchyme-free ureteric bud cultures shows that the rat *Myh7* ortholog can be also induced in the epithelium by recombinant FGF1 or FGF7 (31). The Fgf10 induction of *Myh7* is intriguing and raises the possibility of new unsuspected roles for this myosin in epithelial development.

FGF10 Induces Genes Associated with Inflammatory Responses during Bud Induction

FGF7 activation of Fgfr2b has been shown to modulate interferon-mediated gene expression in adult airway epithelial cell cultures (32). Here we found that among the FGF10 targets with the highest fold induction were genes previously implicated in inflammatory responses and wound healing in other systems. They included the Annexin gene family members, *Anxa1* (110-fold), *Anxa3* (35-fold), and *Anxa2* (4.2-fold) (Table I). Also significantly up-regulated ($p < 0.05$) but not included in our initial list (<3-fold increase) were *Anxa5* (1.9-fold), *Anxa8* (2.5-fold), and *S100A10* (S100 calcium-binding protein A10, 2.8-fold), the partner of *Anxa2*. Annexins are calcium-dependent phospholipid-binding proteins involved in membrane trafficking, cell-matrix interactions, calcium transduction, and inhibition of phospholipase A2. An anti-inflammatory activity has been reported for Annexins, particularly *Anxa1* (33).

Fig. 3, C and D, show that epithelial expression of Annexin genes is dramatically increased by local application of FGF10 protein. By contrast, an analysis of E11.5 lungs showed that distal-proximal gradients of these genes are subtle (*Anxa3*) or not obvious (*Anxa1*) (Fig. 2, D and J) and do not correlate well with the distal gradients of Fgf10-Fgfr2b activity reported in the lung.

This finding indicates that endogenous levels of Fgf10 have only a modest impact on Annexin gene expression. The striking up-regulation of Annexins in our system appears to represent a feedback response of the epithelium to supraphysiological levels of FGF10. Presumably, this mechanism operates in the developing lung to restrict Fgf signaling in conditions in which the Fgf pathway has been hyperactivated by transient increases in ligand production. Indeed, Annexins are potent inhibitors of phospholipase A2 (34), a substrate of activated Fgfr kinase that has been implicated in inflammatory and morphogenetic processes (35).

Other genes associated with inflammatory responses or wound healing up-regulated in our array were: *Tgtp* (T-cell-specific GTPase, 59.6-fold, Fig. 2A), *S100a13* (S100 calcium-binding protein A13, 3.2-fold, Table I), the acute phase response gene *Saa3* (serum amyloid A3, 35-fold, Fig. 2K) and its receptor *Ager* (advanced glycosylation end product-specific receptor, 35-fold, Table I), and *Il10rb* (interleukin 10 receptor β , 4-fold, Table I).

FGF10 Induces Steroid and Lipid Metabolism-related Genes during Epithelial Morphogenesis in Vitro

During morphogenesis, increased lipid synthesis is required for a variety of functions from general processes, such as formation of cellular membranes, to more cell-specific functions, such as surfactant synthesis by the differentiating lung epithelium. Fgf10 is known to be essential for adipogenesis (6–8). FGF signaling stimulates lipogenesis in the developing and adult lung epithelium *in vitro* (36).

Six genes from cluster C, associated with steroid-lipid metabolism, showed a similar pattern of induction by FGF10 (*Ldlr*, *Hsd3b2*, *Lss*, *HSL*, *Cyp51*, and *Scd1* in Table I). At least two of them are known FGF targets involved in lipid synthesis

in cell lines. For example, FGF2 (basic FGF) up-regulates *Ldlr* (low density lipoprotein receptor) in arterial smooth muscle cells to increase LDL uptake (37). The time course of *Ldlr* induction in these cells is similar to that found in our cultures (initial peak at 6–8 h and return to initial levels). FGF7 markedly induces the expression of *Scd1* (stearoyl-coenzyme A desaturase 1) to stimulate surfactant phospholipid synthesis in rat lung type II cells (36). *Scd1* encodes an enzyme required for normal synthesis of triglycerides, cholesterol, and phospholipids (36), which was induced by 4-fold (0–24 h) by FGF10 in our cultures.

In the white adipose tissue, C/EBP α and Fgf10 act synergistically to induce adipocyte differentiation (8). Respiratory dysfunction due to inadequate production of lipids and functional surfactant has been described in C/EBP α null mice (38, 39). C/EBP α was excluded from our original list because signals were only marginally detected in one of the samples. C/EBP α was up-regulated in our array and showed a trend consistent with cluster C (0–8 h, 3-fold; 0–24 h, 1.8-fold; Table I).

Two genes from cluster A associated with lipid metabolism were highly expressed in distal epithelium and responsive to FGF10 in our cultures. They were as follows: *Lrpap1* (HBP44, low density lipoprotein receptor-related protein-associated 1, 0–24 h, 5-fold; Figs. 2M and 3F) and *Cyp1b1* (cytochrome P450, family 1, subfamily B, polypeptide 1, 0–24 h, 15-fold; Figs. 2N and 3E) (40).

Also markedly up-regulated by FGF10 were two genes that have been indirectly implicated in signal transduction via phospholipase C γ /diacylglycerol/calcium, an alternate FGF pathway (35, 41, 42). They were *HSL* (hormone-sensitive lipase, 0–8 h, 12-fold; 0–24 h, 5-fold) and *AHNAK* (*Desmoyokin*, 0–24 h, 25-fold, Table I).

FGF10 Regulation of Genes Associated with Cell Proliferation, Cell Death, and Proteolysis

Although cell cycle-related genes were overrepresented in at least two of our clusters (clusters C and D), most were down-regulated or were only modestly induced by 24 h when budding activity was maximal (Table I, *Cncb1*, *Kif11*, *Mad2l1*, *Cdkn1a*, and *Akap8*). In the case of the cell cycle arrest gene, *Cdkn1a* (*p21*), we found a transient peak (6-fold) in expression during the initial 8h in culture. Kinetic studies indicate that cell proliferation is critical for elongation but not for initiating local budding in the lung epithelium (43). Our gene profiling of the early bud supports these conclusions and suggests that activities such as cell rearrangement and migration, rather than cell proliferation, predominate at earlier stages.

Changes in expression of apoptosis-related genes were unremarkable, in agreement with the overall health status of these cultures and the role of Fgf10 as a survival factor for the developing epithelium. Of interest was the up-regulation of *Porimin* (3.6-fold), a gene encoding a membrane mucin that mediates oncosis, a recently described non-apoptotic mechanism of cell death in cell lines (44). Fig. 2O shows *Porimin* expression in the E11.5 distal lung. Two p53-related genes, *Perp*-pending (*P53* apoptosis effector related to *Pmp22*) and *Prkdc* (protein kinase DNA-activated catalytic polypeptide), implicated in DNA repair were expressed at high levels in our system (13- and 10-fold by 24 h, respectively, Table I).

We identified two genes associated with proteolysis, *Ctsh* (cathepsin H) and *Timp3* (tissue inhibitor of metalloproteinase 3) in distal epithelial buds that were highly induced by FGF10 (35- and 9.3-fold over 24 h, respectively) (Table I and Figs. 2E and 3B and data not shown). *Ctsh* encoded a lysosomal glycoprotein member of the cysteine proteinase family whose function in organogenesis is still unclear (45). The reduced branch-

AQ: F

AQ: G

ing activity reported in *Timp3* null mice suggests a genetic interaction between *Timp3* and *Fgf10* in the developing lung (46). Up-regulation of *Timp3* in our system raises the possibility that one of the functions of FGF10 is to balance metalloproteinase activity in nascent buds.

FGF10 Targets Are Induced in Multiple Developing Organs and in Different Biological Processes

We asked whether the genes identified here as Fgf10 targets in the developing lung were present at other sites that depend on Fgf10 to develop. We found this to be true for several genes, particularly those from cluster A. Fig. 4 shows two examples: *Tacstd2* (tumor-associated calcium signal transducer2; 32-fold increase, 0–24 h), a gene that encodes a cell surface receptor with single-pass transmembrane domain (47), and *Tm4sf3*, the tetraspanin cell adhesion molecule (10.5-fold increase 0–24 h) already described in a previous section.

In situ hybridization analysis of *Tacstd2* in embryos at different stages (E11–14) showed strong signals in putative epithelial cell progenitors of various Fgf10-dependent structures, such as the lung, tooth, hair follicle, skin, renal tubules, ureteric bud, and urogenital sinus (future bladder) (Figs. 2B and 4, A–D). A similar analysis revealed *Tm4sf3* signals in the epithelium of thyroid, lung, stomach, gut, renal tubules, bladder, and tooth. (Fig. 4, I–L). Fig. 4H shows an anterior-posterior gradient of *Tm4sf3* in the E12 stomach remarkably similar to that described for *Fgf10* in the corresponding mesenchyme (48). All of the structures above where these genes were expressed are known to be dramatically altered in *Fgf10* or *Fgfr2b* knock-out mice (5).

The presence of *Tm4sf3* expression in the liver and cartilage primordia of bones (Fig. 4, I, N, and O), structures not reported to be abnormal in these mutant mice (5), suggests an Fgf10-independent regulation of *Tm4sf3* at these sites. Our data suggested that *Tacstd2* has a more specific requirement for Fgf10 than does *Tm4sf3*. The assessment of these genes in whole lung cultures engrafted with FGF-loaded beads showed that *Tm4sf3* is equally up-regulated by FGF10 or FGF7. However, *Tacstd2* responded only to FGF10 (Fig. 4, E–G and P–R). This is intriguing, because these FGFs utilize the same receptor for signaling (49).

It is long believed that organogenesis and tumorigenesis share common features and regulatory pathways. Interestingly, *Tacstd2* and *Tm4sf3* have been recognized as tumor antigens and are associated with tumor invasion and metastatic behavior. *Tacstd2* has been reported in tumors of various origins, including prostate and mammary gland (50). Increased levels of *Tm4sf3* have been reported in several metastatic carcinomas (51–53). *Tm4sf3* regulates cell migration by modulating integrin compartmentalization and signaling. *Tm4sf3* co-expression with $\alpha_6\beta_4$ integrin induces a motile phenotype and triggers metastatic spread in several rat tumor cell lines (54). It is possible that, in our system, activation of these tumor-associated genes by Fgf10-Fgfr2b confers an invasive and presumably less differentiated phenotype to the epithelium during bud morphogenesis.

Summary and Concluding Remarks

We used DNA microarray and *in situ* hybridization approaches to identify transcriptional targets of Fgf10 in the developing epithelium during bud morphogenesis. The screen was targeted to the initial stages of bud formation and was designed to identify the earliest transcriptional events downstream Fgfr2b activation during this process. Our analysis revealed up-regulation of a large number of genes associated with cell rearrangement and migration, inflammatory pro-

cesses, and lipid metabolism. The modest changes observed in cell cycle-related genes were consistent with the idea that cell proliferation does not play a major role in initiation of budding (43).

Genetic data indicate that during organogenesis Fgf10-Fgfr2b signaling is required for bud formation in multiple developing structures (3–5). Thus, the Fgf targets identified in our screen are likely to be relevant for budding in other organs. The confirmation of selected genes in various structures that depend on Fgf10-Fgfr2 to develop favors this hypothesis.

A number of studies support a role for Fgf10 in maintaining a progenitor-like state of a population of epithelial cells during organ development (20, 55–57). Here we were unable to clearly identify a subset of Fgf10 target genes characteristic of this state. This reflects some of the current difficulties in defining the markers for these progenitor cells. Perhaps the target genes, such as *Tactds2* and *Tm4sf1*, present in relatively undifferentiated epithelial cells during both development and cancer are representative of these markers.

Acknowledgments—We thank Lan Wei in the Microarray Core Facility of Tufts University for providing us the cDNA clones and PCR products. We thank Jan Blusztajn and Stephen Farmer for helpful discussion. We are also grateful to Xiaoqian Qi and Chun Li for technical assistance.

REFERENCES

- Orr-Urtreger, A., Bedford, M. T., Burakova, T., Arman, E., Zimmer, Y., Yayon, A., Givol, D., and Lonai, P. (1993) *Dev. Biol.* **158**, 475–486
- Sekine, K., Ohuchi, H., Fujiwara, M., Yamasaki, M., Yoshizawa, T., Sato, T., Yagishita, N., Matsui, D., Koga, Y., Itoh, N., and Kato, S. (1999) *Nat. Genet.* **21**, 138–141
- Arman, E., Haffner-Krausz, R., Gorivodsky, M., and Lonai, P. (1999) *Proc. Natl. Acad. Sci. U. S. A.* **96**, 11895–11899
- De Moerloose, L., Spencer-Dene, B., Revest, J., Hajihosseini, M., Rosewell, I., and Dickson, C. (2000) *Development* **127**, 483–492
- Ohuchi, H., Hori, Y., Yamasaki, M., Harada, H., Sekine, K., Kato, S., and Itoh, N. (2000) *Biochem. Biophys. Res. Commun.* **277**, 643–649
- Sakaue, H., Konishi, M., Ogawa, W., Asaki, T., Mori, T., Yamasaki, M., Takata, M., Ueno, H., Kato, S., Kasuga, M., and Itoh, N. (2002) *Genes Dev.* **16**, 908–912
- Tagashira, S., Harada, H., Katsumata, T., Itoh, N., and Nakatsuka, M. (1997) *Gene (Amst.)* **197**, 399–404
- Asaki, T., Konishi, M., Miyake, A., Kato, S., Tomizawa, M., and Itoh, N. (2004) *Mol. Cell. Endocrinol.* **218**, 119–128
- Bellucci, S., Grindley, J., Emoto, H., Itoh, N., and Hogan, B. L. (1997) *Development* **124**, 4867–4878
- Park, W. Y., Miranda, B., Lebeche, D., Hashimoto, G., and Cardoso, W. V. (1998) *Dev. Biol.* **201**, 125–134
- Wertz, K., and Herrmann, B. G. (2000) *Mech. Dev.* **98**, 51–70
- Cardoso, W. V., Itoh, A., Nogawa, H., Mason, I., and Brody, J. S. (1997) *Dev. Dyn.* **208**, 398–405
- Lu, J., Qian, J., Izvolsky, K. I., and Cardoso, W. V. (2004) *Dev. Biol.* **273**, 418–435
- Garcia-Montero, A., Vasseur, S., Mallo, G. V., Soubeyran, P., Dagorn, J. C., and Iovanna, J. L. (2001) *Eur. J. Cell Biol.* **80**, 720–725
- Lebeche, D., Malpel, S., and Cardoso, W. V. (1999) *Mech. Dev.* **86**, 125–136
- Weaver, M., Dunn, N. R., and Hogan, B. L. (2000) *Development* **127**, 2695–2704
- Nelson, W. J., and Nusse, R. (2004) *Science* **303**, 1483–1487
- Okubo, T., and Hogan, B. L. (2004) *J. Biol.* **3**, 11
- Israsena, N., Hu, M., Fu, W., Kan, L., and Kessler, J. A. (2004) *Dev. Biol.* **268**, 220–231
- Tao, H., Yoshimoto, Y., Yoshioka, H., Nohno, T., Noji, S., and Ohuchi, H. (2002) *Mech. Dev.* **116**, 39–49
- Sato, M., and Kornberg, T. B. (2002) *Dev. Cell* **3**, 195–207
- Berditchevski, F. (2001) *J. Cell Sci.* **114**, 4143–4151
- Knoblich, J. A., Jan, L. Y., and Jan, Y. N. (1997) *Cold Spring Harbor Symp. Quant. Biol.* **62**, 71–77
- Fischer, R. S., Fritz-Six, K. L., and Fowler, V. M. (2003) *J. Cell Biol.* **161**, 371–380
- Aurrand-Lions, M., Galland, F., Bazin, H., Zakharyev, V. M., Imhof, B. A., and Naquet, P. (1996) *Immunity* **5**, 391–405
- Grimmond, S., Van Hateren, N., Siggers, P., Arkell, R., Larder, R., Soares, M. B., de Fatima, B. M., Smith, L., Tymowska-Lalanne, Z., Wells, C., and Greenfield, A. (2000) *Hum. Mol. Genet.* **9**, 1553–1560
- Ooshio, T., Irie, K., Morimoto, K., Fukuhara, A., Imai, T., and Takai, Y. (2004) *J. Biol. Chem.* **279**, 31365–31373
- Wertz, K., and Herrmann, B. G. (1999) *Mech. Dev.* **84**, 185–188
- Bertet, C., Sulak, L., and Lecuit, T. (2004) *Nature* **429**, 667–671
- Lyons, G. E., Ontell, M., Cox, R., Sassoon, D., and Buckingham, M. (1990) *J. Cell Biol.* **111**, 1465–1476
- Qiao, J., Bush, K. T., Steer, D. L., Stuart, R. O., Sakurai, H., Wachsman, W., and Nigam, S. K. (2001) *Mech. Dev.* **109**, 123–135
- Prince, L. S., Karp, P. H., Moninger, T. O., and Welsh, M. J. (2001) *Physiol.*

AQ: H

AQ: I

AQ: J

- Genomics* **6**, 81–89
33. Gerke, V., and Moss, S. E. (2002) *Physiol. Rev.* **82**, 331–371
34. Wallner, B. P., Mattaliano, R. J., Hession, C., Cate, R. L., Tizard, R., Sinclair, L. K., Foeller, C., Chow, E. P., Browning, J. L., and Ramachandran, K. L. (1986) *Nature* **320**, 77–81
35. Kondo, H., and Yonezawa, Y. (2000) *Biochem. Biophys. Res. Commun.* **272**, 648–652
36. Mason, R. J., Pan, T., Edeen, K. E., Nielsen, L. D., Zhang, F., Longphre, M., Eckart, M. R., and Neben, S. (2003) *J. Clin. Investig.* **112**, 244–255
37. Hsu, H. Y., Nicholson, A. C., and Hajjar, D. P. (1994) *J. Biol. Chem.* **269**, 9213–9220
38. Flodby, P., Barlow, C., Kylefjord, H., Ahrlund-Richter, L., and Xanthopoulos, K. G. (1996) *J. Biol. Chem.* **271**, 24753–24760
39. Sugahara, K., Iyama, K. I., Kimura, T., Sano, K., Darlington, G. J., Akiba, T., and Takiguchi, M. (2001) *Cell Tissue Res.* **306**, 57–63
40. Jansson, I., Stoilov, I., Sarfarazi, M., and Schenkman, J. B. (2001) *Pharmacogenetics* **11**, 793–801
41. Williams, R. L., and Katan, M. (1996) *Structure* **4**, 1387–1394
42. Sekiya, F., Bae, Y. S., Jhon, D. Y., Hwang, S. C., and Rhee, S. G. (1999) *J. Biol. Chem.* **274**, 13900–13907
43. Nogawa, H., Morita, K., and Cardoso, W. V. (1998) *Dev. Dyn.* **213**, 228–235
44. Zhang, C., Xu, Y., Gu, J., and Schlossman, S. F. (1998) *Proc. Natl. Acad. Sci. U. S. A.* **95**, 6290–6295
45. Turk, V., Turk, B., and Turk, D. (2001) *EMBO J.* **20**, 4629–4633
46. Gill, S. E., Pape, M. C., Khokha, R., Watson, A. J., and Leco, K. J. (2003) *Dev. Biol.* **261**, 313–323
47. Ripani, E., Sacchetti, A., Corda, D., and Alberti, S. (1998) *Int. J. Cancer* **76**, 671–676
48. Aubin, J., Dery, U., Lemieux, M., Chailier, P., and Jeannotte, L. (2002) *Development* **129**, 4075–4087
49. Szebenyi, G., and Fallon, J. F. (1999) *Int. Rev. Cytol.* **185**, 45–106
50. Fornaro, M., Dell’Arciprete, R., Stella, M., Bucci, C., Nutini, M., Capri, M. G., and Alberti, S. (1995) *Int. J. Cancer* **62**, 610–618
51. Kanetaka, K., Sakamoto, M., Yamamoto, Y., Yamasaki, S., Lanza, F., Kanematsu, T., and Hirohashi, S. (2001) *J. Hepatol.* **35**, 637–642
52. Kanetaka, K., Sakamoto, M., Yamamoto, Y., Takamura, M., Kanematsu, T., and Hirohashi, S. (2003) *J. Gastroenterol. Hepatol.* **18**, 1309–1314
53. Huerta, S., Harris, D. M., Jazirehi, A., Bonavida, B., Elashoff, D., Livingston, E. H., and Heber, D. (2003) *Int. J. Oncol.* **22**, 663–670
54. Herlevsen, M., Schmidt, D. S., Miyazaki, K., and Zoller, M. (2003) *J. Cell Sci.* **116**, 4373–4390
55. Norgaard, G. A., Jensen, J. N., and Jensen, J. (2003) *Dev. Biol.* **264**, 323–338
56. Harada, H., Toyono, T., Toyoshima, K., and Ohuchi, H. (2002) *Connect. Tissue Res.* **43**, 201–204
57. Bhushan, A., Itoh, N., Kato, S., Thiery, J. P., Czernichow, P., Bellusci, S., and Scharfmann, R. (2001) *Development* **128**, 5109–5117

